

Communication

Correlation of Crystal Defects with Device Performance of AlGa_N/Ga_N High-Electron-Mobility Transistors Fabricated on Silicon and Sapphire Substrates

Sakhone Pharkphoumy¹, Vallivedu Janardhanam¹ , Tae-Hoon Jang², Kyu-Hwan Shim^{1,2,*} and Chel-Jong Choi^{1,*}

¹ School of Semiconductor and Chemical Engineering, Semiconductor Physics Research Center, Jeonbuk National University, Jeonju 54896, Republic of Korea

² R&D Center, Sigetronics Inc., Jeonbuk 55314, Republic of Korea

* Correspondence: khshim@jbnu.ac.kr (K.-H.S.); cjchoi@jbnu.ac.kr (C.-J.C.)

Abstract: Herein, the performance of AlGa_N/Ga_N high-electron-mobility transistor (HEMT) devices fabricated on Si and sapphire substrates is investigated. The drain current of the AlGa_N/Ga_N HEMT fabricated on sapphire and Si substrates improved from 155 and 150 mA/mm to 290 and 232 mA/mm, respectively, at $V_{GS} = 0$ V after SiO₂ passivation. This could be owing to the improvement in the two-dimensional electron gas charge and reduction in electron injection into the surface traps. The SiO₂ passivation resulted in the augmentation of breakdown voltage from 245 and 415 V to 400 and 425 V for the AlGa_N/Ga_N HEMTs fabricated on Si and sapphire substrates, respectively, implying the effectiveness of SiO₂ passivation. The lower transconductance of the AlGa_N/Ga_N HEMT fabricated on the Si substrate can be ascribed to the higher self-heating effect in Si. The X-ray rocking curve measurements demonstrated that the AlGa_N/Ga_N heterostructures grown on sapphire exhibited a full-width half maximum of 368 arcsec against 703 arcsec for the one grown on Si substrate, implying a better crystalline quality of the AlGa_N/Ga_N heterostructure grown on sapphire. The AlGa_N/Ga_N HEMT fabricated on the sapphire substrate exhibited better performance characteristics than that on the Si substrate, owing to the high crystalline quality and improved surface.

Keywords: AlGa_N/Ga_N HEMT; defects; silicon; sapphire; breakdown voltage; passivation



Citation: Pharkphoumy, S.; Janardhanam, V.; Jang, T.-H.; Shim, K.-H.; Choi, C.-J. Correlation of Crystal Defects with Device Performance of AlGa_N/Ga_N High-Electron-Mobility Transistors Fabricated on Silicon and Sapphire Substrates. *Electronics* **2023**, *12*, 1049. <https://doi.org/10.3390/electronics12041049>

Academic Editor: Wojciech Wojtasiak

Received: 16 January 2023
Revised: 13 February 2023
Accepted: 17 February 2023
Published: 20 February 2023



Copyright: © 2023 by the authors. Licensee MDPI, Basel, Switzerland. This article is an open access article distributed under the terms and conditions of the Creative Commons Attribution (CC BY) license (<https://creativecommons.org/licenses/by/4.0/>).

1. Introduction

Group III nitride-based heterostructures have attracted considerable interest for their promising applications in the development of high-performance high-electron-mobility transistors (HEMTs), ultraviolet light-emitting diodes, optical data storage, and related devices because of their large band gap, high bulk mobility, and high critical field strength [1–5]. In particular, AlGa_N/Ga_N heterostructures are extensively employed in HEMTs for high-frequency and high-power devices, as well as in biological and chemical sensors and piezotronics [6,7]. In AlGa_N/Ga_N HEMTs, the two-dimensional electron gas (2DEG) is originated due to the spontaneous and piezoelectric polarization induced sheet charge formed at the AlGa_N/Ga_N heterojunction [8,9]. Owing to the high-cost and availability limitation of III-nitride bulk substrates, the epitaxial layers were grown on foreign substrates such as SiC, diamond, Si, and sapphire for Ga_N-based HEMT devices fabrication [10,11]. However, the specific substrates used for the growth of epitaxial nitride structures rely on specific applications. Sapphire substrate suffers from a low thermal conductivity and higher defect density owing to its large lattice mismatch degrading the high-power operation of transistor devices. SiC exhibits a lesser lattice mismatch to Ga_N and a higher thermal conductivity than sapphire, however, it is hindered due to its expensiveness and availability limitation particularly for the electrically insulating 4H-SiC [6]. Si is a promising alternate

for the growth of III-nitrides due to its inexpensiveness, high-quality, large-area obtainability, and the opportunity of integrability of GaN-based high-power devices with Si-based devices [12,13]. Silicon exhibits a higher thermal conductivity than sapphire and similar to that of GaN, and the well-developed processing techniques make Si a very attractive substrate for high-power III-nitride applications [12,13]. However, the main challenge with using Si is the high thermal expansion and lattice mismatch coefficients as compared with the III-nitrides that necessitate the use of thick buffers prior to the growth of GaN so as to decrease the threading dislocations density. The lattice mismatch amid GaN and the substrates used for GaN growth is a key concern. This mismatch might affect crystallization, resulting in the generation of defects/threading dislocations causing a large surface leakage current thereby consequently degrading the device performance. Nevertheless, the GaN buffer layer growth with high-structural-quality that enables good crystallization with minimum defects and a smooth film surface is crucial for the development of high-performance GaN-based devices [1]. Several methods have been proposed to enhance the GaN material growth with regard to dislocation density such as the insertion of interlayers, optimization of nucleation layers, annealing step growth in silane, two-step growth, and epitaxial lateral overgrowth and its modifications [11,14–16]. Furthermore, considerable research has been performed to optimize the GaN buffer layer thickness, AlGaIn active layer thickness, and the composition of Al in the AlGaIn layer towards achieving an improved performance in AlGaIn/GaN HEMTs [17–19].

Although there have been several reports on large-current and high-voltage AlGaIn/GaN HEMTs, the surface leakage current is still high and the on-off current ratio is inadequate for high-efficiency power devices. The electrons injection from the channel to the surface states of the AlGaIn/GaN heterostructure degrades the electrical properties of AlGaIn/GaN HEMTs, such as the forward drain current (I_{DS}), leakage current, and breakdown voltage [20,21]. Several surface passivation methods for these surface states using SiO_2 , Si_3N_4 , Sc_2O_3 , and benzocyclobutene have been investigated [21–26]. The passivation enhances the DC characteristics and reduces the RF dispersion of AlGaIn/GaN HEMTs. SiO_2 passivation has been reported in voltage-switching GaN devices and it reduced the current leakage in GaN Schottky barrier detectors and the AlGaIn/GaN metal-oxide-semiconductor field-effect transistor [27,28]. Although, there are several reports available on the SiO_2 passivation mechanism for high-voltage switching in AlGaIn/GaN HEMTs [28–30], to the best of our knowledge, the reports available on a comparison of SiO_2 passivation of AlGaIn/GaN HEMTs on Si and sapphire substrates are scarce.

In this work, a systematic investigation was performed to study the effects of sapphire (Al_2O_3) and Si substrates on the growth of AlGaIn/GaN HEMT structures with an exploration on the influence of SiO_2 passivation of the surface on the electrical characteristics of AlGaIn/GaN HEMTs grown on Si and sapphire substrates and compared with those of unpassivated HEMTs. The electrical characteristics of unpassivated AlGaIn/GaN HEMTs were studied and correlated with their structural properties. The AlGaIn/GaN HEMT grown on sapphire exhibited better DC performance with improved drain current density compared with the HEMT on Si substrate. Moreover, the performances of the HEMTs fabricated on both Si and sapphire substrates enhanced after passivation. The breakdown voltage (V_{BR}) of the AlGaIn/GaN HEMTs enhanced after SiO_2 passivation. However, a significant improvement in V_{BR} was observed in the HEMT fabricated on Si substrate. The X-ray diffraction rocking curve results further demonstrated that the heterostructure deposited on the sapphire substrate exhibits good crystalline quality with a 002 reflection peak with a full-width half maximum (FWHM) of 0.13° against an FWHM of 0.20° for the heterostructure grown on a Si substrate. The outcomes of this work could indeed provide a better insight for the implementation of AlGaIn/GaN HEMTs with improved performance.

2. Materials and Methods

In this work, the metal organic chemical vapor deposition (MOCVD) grown epitaxial wafers on Si and sapphire substrates were purchased from Nippon Telegraph and Tele-

phone Advanced Technology Co. (NNT-AT), Japan. The epitaxial wafers comprised, a 2- μm -thick GaN buffer layer with carbon-doping, a 300-nm-thick undoped GaN (i-GaN) layer, and a 23-nm-thick AlGaIn barrier layer with aluminum composition of 25%. A 2DEG channel with an electron mobility of $1700\text{ cm}^2/\text{V}\cdot\text{s}$ and a sheet electron density of $1.1 \times 10^{13}\text{ cm}^{-2}$ was formed at the polarized AlGaIn/GaN heterostructure interface. The choice of 25% aluminum, 300-nm-thick GaN channel, and 23-nm-AlGaIn layer thickness are considered for the growth of AlGaIn/GaN heterostructure to obtain high-performance AlGaIn/GaN HEMTs through maintaining a trade-off between the on-current and the channel breakdown based on the 2DEG and the energy band gap. Further, the thickness of the layers is selected to obtain reduced deep traps, reduced threading dislocations, and reduced electron capture probability by the deep traps [31]. Both AlGaIn/GaN HEMT device structures were processed under the same processing conditions, as exhibited in flow chart in Figure 1a. First, the wafers were cleaned using acetone followed by isopropyl alcohol for a duration of 3 min each. All cleanings were performed using ultrasonic agitation for the removal of organic contaminants from the surface. Later, the wafers were dipped in a $\text{H}_2\text{SO}_4 + \text{H}_2\text{O}_2$ (1:1) solution for 20 min and then in a buffer oxide etch (BOE) solution for 2 min. The cleaning procedure is an important step in preparing a surface for the formation of intimate electrode contact with the semiconductor. Mesa etching of the AlGaIn/GaN layer was accomplished using an inductively coupled plasma (ICP) plasma-therm system defined by a photoresist hard mask with Ar/ Cl_2 / BCl_3 gas mixtures at an RF/bias power of 200/50 W and a chamber pressure of 3 mTorr. Ti/Al/Ni/Au (200/800/500/1000 Å) ohmic electrodes were formed as source and drain contacts by electron-beam evaporation tracked by rapid-thermal-annealing at $850\text{ }^\circ\text{C}$ for 1 min in N_2 flow. The sheet resistance and contact resistance values of $400.21\text{ }\Omega/\text{cm}^2$ and $24.5\text{ }\Omega$, $666.84\text{ }\Omega/\text{cm}^2$, and $20.97\text{ }\Omega$ were obtained from the transmission line models (TLM) on Si and sapphire substrate, respectively. Finally, a Schottky gate contact was fabricated by the electron-beam evaporation of Ni/Au (200/1000 Å) films, defined by the pattern using standard UV lithography. To investigate the surface passivation effect using SiO_2 on the AlGaIn/GaN HEMT characteristics, a 200 nm thick SiO_2 passivation layer was deposited on the fabricated HEMT structures via plasma-enhanced chemical vapor deposition. Prior to oxide passivation, the devices were cleaned by a BOE surface treatment for 1 min. The deposited SiO_2 is sufficiently thick to create an electric field in the channel to reach the drain. Later, the source/drain and gate contact regions were opened by BOE etching. Schematics of the fabricated AlGaIn/GaN structures with and without SiO_2 passivation are exhibited in Figure 1b,c, respectively. The output and transfer characteristics of the fabricated AlGaIn/GaN HEMTs were measured with a precision semiconductor parameter analyzer (Agilent 4156 C). The structural characterization of the AlGaIn/GaN heterostructures grown on Si and sapphire substrates were performed employing high-resolution X-ray diffraction (HR-XRD, PANalytical X'Pert Pro MRD). The root-mean-square surface roughness of the structures was measured by atomic force microscope (AFM; n-tracer, NanoFocus, Oberhausen, Germany).

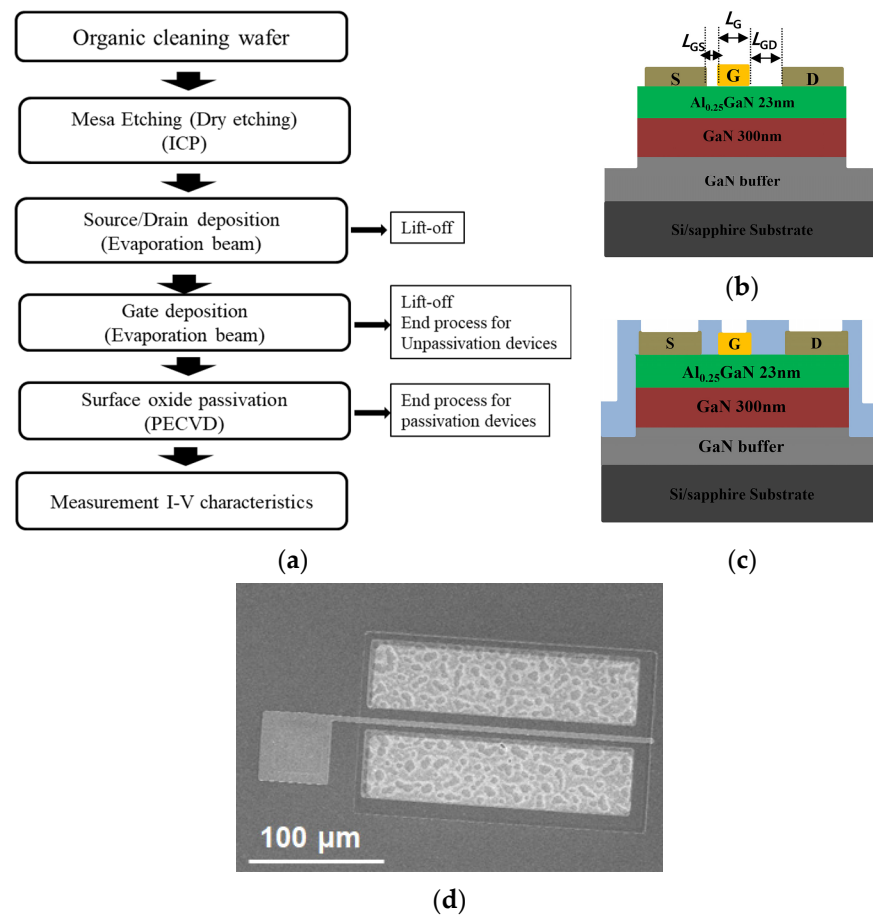


Figure 1. (a) Flow chart showing the device fabrication process, schematic of the fabricated AlGaIn/GaN HEMTs (b) without and (c) with SiO₂ passivation, lengths are similar of $L_{GS} = 4\mu\text{m}$, $L_G = 4.5\mu\text{m}$, and $L_{GD} = 10\mu\text{m}$, respectively, (d) scanning electron microscope image of the fabricated AlGaIn/GaN HEMT structure.

3. Results and Discussion

Figure 2a,b exhibit the output ($I_{DS}-V_{DS}$) curves of AlGaIn/GaN HEMTs grown on Si and sapphire substrates at various V_{GS} values varying in the range of -4 to 0 V with and without SiO₂ passivation, respectively. The AlGaIn/GaN HEMT grown on sapphire without any passivation shows better DC performance with a high drain current density of 155 mA/mm at $V_{GS} = 0\text{ V}$ than the HEMT grown on Si, which displayed a high drain current density of 150 mA/mm . However, the performance of the AlGaIn/GaN HEMT fabricated on the passivated surfaces of both sapphire and Si substrates improved with drain current densities of 290 and 232 mA/mm at $V_{GS} = 0\text{ V}$, respectively. The low drain current for low gate voltages (V_{GS}) is associated with the reduced carriers in the heterojunction. The improvement in the drain currents after SiO₂ passivation could be ascribed to the increase in the 2DEG charge and decrease in the electron injection to the surface traps [28]. Passivation decreases the surface effects that in turn augments the carriers in the channel leading to an increase in the drain current [32]. It can be noted that the drain current is higher for the AlGaIn/GaN HEMTs fabricated on the sapphire than on the Si substrate that were identically processed and is mainly the effect of the substrates. Owing to the fact that both the devices have identical active layers, this higher drain current for the AlGaIn/GaN HEMT on sapphire could be due to the better crystallinity than the Si sample that will be shown in the later sections [33]. The AlGaIn/GaN HEMT fabricated on a passivated sapphire exhibited maximum values of I_{DS} at $V_{DS} = 5\text{ V}$ and $V_{GS} = 0\text{ V}$. It is to be noted that I_{DS} decreased with increasing V_{DS} owing to the self-heating effect of the sapphire because of its low thermal conductivity that limits the output power of the fabricated AlGaIn/GaN

HEMT [10,34,35]. Self-heating results in an increase in channel temperature that not only decreases the electron mobility and saturation velocity but also reduces the median time of power devices failure [35,36]. However, for AlGaIn/GaN HEMT fabricated on passivated silicon, the decrease in I_{DS} is negligible, implying a higher thermal conductivity of the Si than that of the sapphire substrate [10,34].

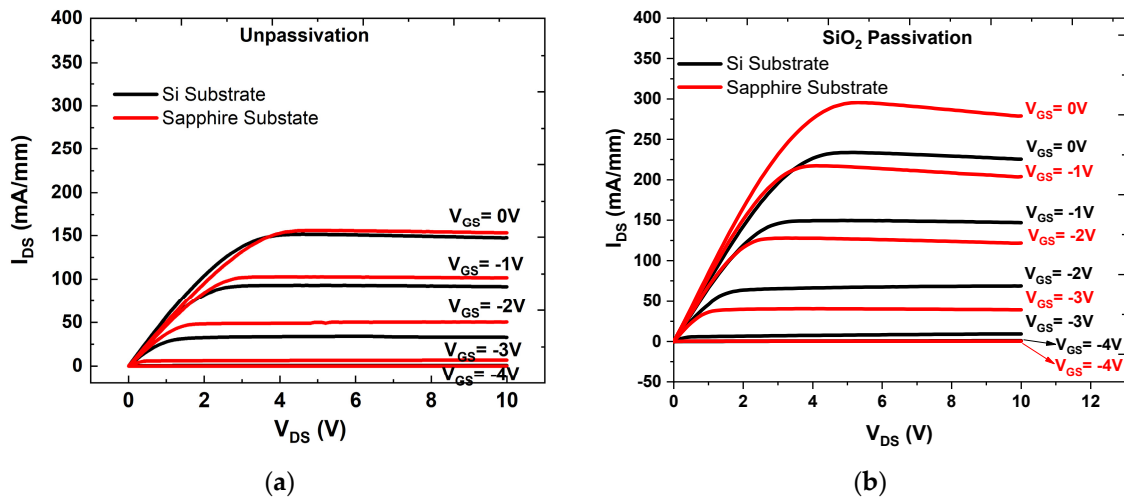


Figure 2. On-state I_{DS} - V_{DS} curves of AlGaIn/GaN HEMTs on Si and sapphire substrates (a) without and (b) with SiO_2 passivation.

Figure 3a,b exhibit the breakdown voltage (V_{BR}) curves of the AlGaIn/GaN HEMTs fabricated on Si and sapphire substrates with and without SiO_2 passivation, respectively. V_{BR} is defined as V_{DS} at $I_G = 1$ mA at a gate bias $V_{GS} = -10$ V. The drain-gate leakage current limits the V_{BR} in these devices. For the AlGaIn HEMTs fabricated on Si and sapphire substrates without any surface passivation, the V_{BR} is obtained as 245 and 415 V, respectively, at corresponding gate leakage currents (I_G) of 10 μA and 10 nA. The V_{BR} values increased to 400 and 425 V after SiO_2 passivation of the Si and sapphire substrates, respectively. The increase was owing to the decreased surface leakage current associated with electron injection suppression to the surface traps, implying the effectiveness of the SiO_2 passivation [28]. It is worth noting that the V_{BR} increased about 40% and by only 4%, respectively, for the AlGaIn/GaN HEMTs fabricated on Si and sapphire substrates with SiO_2 passivation. The V_{BR} increased only slightly after SiO_2 passivation for the AlGaIn/GaN HEMT on sapphire substrate as compared with the one on Si that were processed identically. This slight increase in V_{BR} could be due to the poorer thermal conductivity of sapphire. Self-heating happens as the applied power to the device produces heat that is not effectively conducted away letting the device to remain at the substrate's ambient temperature. As the drain voltage is increased, the self-heating effects increases the device's lattice temperature degrading the physical properties thus limiting the device V_{BR} . As shown in Figure 3b, I_G increased slightly after SiO_2 passivation, particularly in the case of the HEMT fabricated on the Si substrate. This could be associated with the screening of traps, thereby enhancing the 2DEG [28,37].

Figure 4a,b exhibit the transfer and transconductance curves at $V_{DS} = 10$ V for the AlGaIn/GaN HEMTs fabricated on Si and sapphire substrates with and without SiO_2 passivation. It is to be noted that the threshold voltage (V_{th}) decreases after oxide passivation with a shift towards the negative side from -3.0 to -3.5 V and from -3.0 to -3.8 V for the AlGaIn/GaN HEMTs fabricated on Si and sapphire substrates, respectively. The decrease in V_{th} after SiO_2 passivation could be due to reduction of electron trapping in the surface states [38,39]. Furthermore, from the figures, it can be noticed that a high transconductance ($g_{m,max}$) of 50 and 58 mS/mm for the AlGaIn/GaN HEMTs fabricated on Si and sapphire substrates increases to 80 and 86 mS/mm after SiO_2 passivation, respectively, at $V_{DS} = 10$ V. This increase in $g_{m,max}$ is associated with an increase in I_{DS} . It can be noticed that the

g_m of the AlGaIn/GaN HEMT on sapphire substrate is larger than that of the HEMT on Si for lower V_{GS} till -2 and -0.9 V, respectively, for the HEMTs without and with SiO_2 passivation at which the g_m crosses each other. The behavior of g_m changes after this crossing such that the g_m of the AlGaIn/GaN HEMT on sapphire is lower than the one fabricated on Si substrate. Further, the g_m of the AlGaIn/GaN HEMT decreases rapidly after this crossing particularly in the case of the HEMT fabricated on sapphire substrate owing to the self-heating effect as discussed earlier.

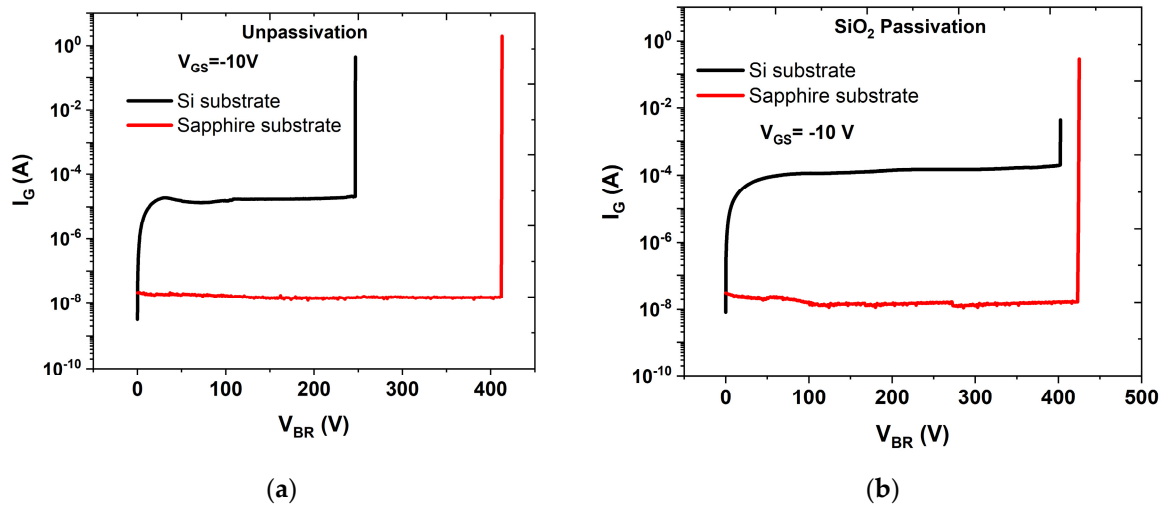


Figure 3. The off-state I_{GS} - V_{DS} curves of AlGaIn/GaN HEMTs on Si and sapphire substrates (a) without and (b) with SiO_2 passivation.

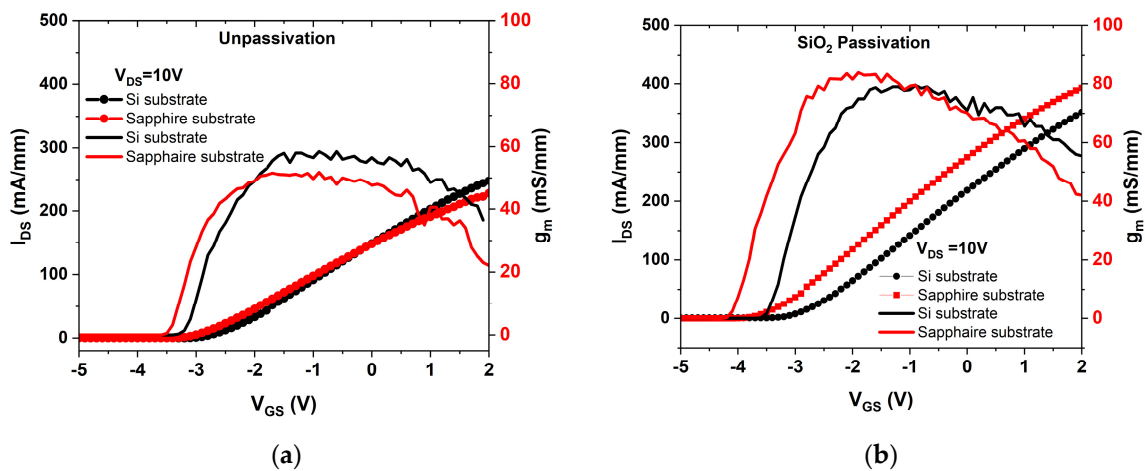


Figure 4. The I_{DS} - V_{GS} transfer curves and transconductance curves of AlGaIn/GaN HEMTs on Si and sapphire substrates (a) without and (b) with SiO_2 passivation.

Figure 5 exhibits the linear output (I_{DS} - V_{DS}) curves of AlGaIn/GaN HEMTs fabricated on Si and sapphire substrates with and without SiO_2 passivation at $V_{GS} = 0$ V, with which the dynamic resistance (R_{ON}) was determined. The R_{ON} reflects charge trapping in the material and is accredited to the interface trap states, barrier, surface, and buffer layer [40]. The values of R_{ON} are 4.44 and 4.33 $\Omega \cdot mm$ for the AlGaIn/GaN HEMTs fabricated on Si and sapphire substrates without SiO_2 passivation and obtained as 0.64 $\Omega \cdot mm$ and 1.26 $\Omega \cdot mm$ for the HEMTs fabricated on SiO_2 passivated surfaces. It was clearly observed that R_{ON} decreased after SiO_2 passivation. This decrease in R_{ON} possibly indicates the effectiveness of the passivation and could be associated with the increase in the 2DEG and the suppression of electron injection into the surface traps [28].

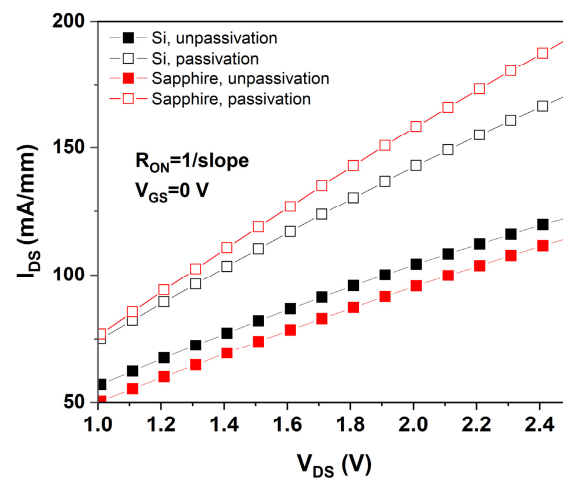


Figure 5. Plot showing the linear regime of I_{DS} versus V_{DS} curves at $V_{GS} = 0$ V for determining the dynamic on resistance of AlGaIn/GaN HEMTs on Si and sapphire substrates without and with SiO_2 passivation.

The structural quality of the AlGaIn/GaN epilayers grown on Si and sapphire substrates was investigated in the $2\theta/\omega$ scan mode using high-resolution X-ray diffraction (HR-XRD) to elucidate its effect on the device behavior of AlGaIn/GaN HEMT. Figure 6a,b show the XRD ω -scan rocking curves of the (002) and (004) planes. The full width at half maximum (FWHM) values of the 002 and 004 diffraction peaks of AlGaIn/GaN grown on both Si and sapphire substrates are presented in Table 1. From the measurements, the heterostructure deposited on the sapphire substrate exhibited good crystalline quality with a 002 reflection peak with an FWHM of 368 arcsec against an FWHM of 720 arcsec for the heterostructure grown on the Si substrate. The difference in the quality of the material depends mainly on the lattice mismatch and the crystal structure between the substrates and nitrides. In addition, the thermal expansion coefficient mismatch limits the material quality, resulting in residual strain with regard to epitaxy and dislocations [6,41]. Tensile stress is created in the heterostructures grown on Si and sapphire substrates owing to the variance in the thermal coefficients of the substrate materials and GaN. From the XRD results, it was noticed that the GaN grown on the sapphire substrate had a good crystalline quality. Figure 6c,d depict the optical force microscope images displaying the topography of the AlGaIn/GaN epilayers grown on the Si and sapphire substrates. It is clearly observed from Figure 6c that the AlGaIn epilayer grown on the Si substrate exhibits a large number of surface pits that may arise because of the threading dislocations intersection with the surface [1,42]. Furthermore, the surface topography of the GaN epilayers grown on Si and sapphire substrates was examined using atomic force microscopy (AFM) (Figures not shown here). A root-mean-square surface roughness of 2.96 and 0.88 nm is obtained from the AFM measurements for the GaN epilayers grown on Si and sapphire substrates, respectively, implying the GaN epilayer grown on sapphire exhibited a smooth surface. From the XRD and AFM results obtained, the AlGaIn/GaN grown on the sapphire substrate exhibits better quality than that on a Si substrate owing to the larger lattice mismatch of GaN with Si compared with the sapphire substrate [41,43]. Lattice mismatch leads to high defect density and structural defects. Structural properties such as crystal quality, defects, and traps of the substrates affect the electrical properties of the fabricated devices. Owing to its better structural properties, the AlGaIn/GaN HEMT grown on a sapphire substrate exhibited better electrical properties than those grown on a Si substrate.

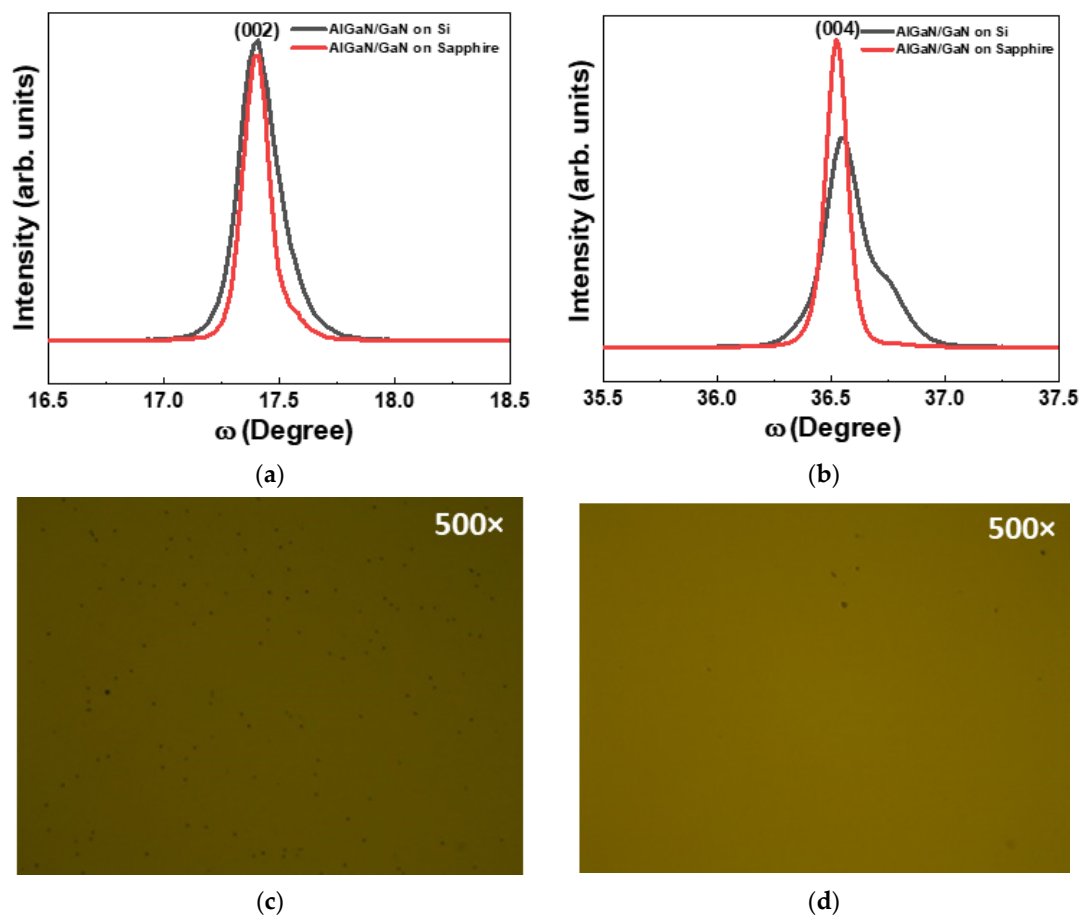


Figure 6. ω -scan rocking curves of (a) (002) and (b) (004) planes, optical microscope images of AlGaIn/GaN surface grown on (c) Si and (d) sapphire.

Table 1. Parameters of the AlGaIn/GaN grown on different substrates.

Substrates	R_a (nm)	HR-XRD 002 FWHM (Degree)	HR-XRD 004 FWHM (Degree)	XRC 002 FWHM (Arcsec)	XRC 102 FWHM (Arcsec)
AlGaIn/GaN-on-Silicon	2.96	0.20	0.23	720	1312
AlGaIn/GaN-on-sapphire	0.88	0.13	0.12	368	647

R_a is roughness average.

4. Conclusions

The performance characteristics of the AlGaIn/GaN HEMT structures fabricated on sapphire and Si substrates with and without SiO₂ passivation were investigated. SiO₂ passivation of the AlGaIn/GaN HEMT led to an augmentation in the drain current I_{DS} which could be attributed with an enhancement in the 2DEG charge and a decrease in the electron injection into the surface traps. The breakdown voltage of the HEMT increased on SiO₂ passivation because of a reduction in the surface leakage current, indicating the effectiveness of SiO₂ passivation. This implies that SiO₂ passivation provides an effective approach for enhancing the electrical behavior of AlGaIn/GaN HEMTs. The AlGaIn/GaN HEMT device grown on a sapphire substrate displayed improved electrical performance compared with that grown on a Si substrate, which could be associated with the better crystallinity of the AlGaIn/GaN heterostructure on sapphire. The outcomes of this work could indeed deliver an approach for the selection of the substrates for III-nitride epitaxial layers growth and surface passivation for the implementation of high performance AlGaIn/GaN HEMTs on the basis.

Author Contributions: Conceptualization, S.P. and V.J.; methodology, S.P.; formal analysis, S.P., V.J. and T.-H.J.; writing—original draft preparation, S.P.; writing—review and editing, K.-H.S. and C.-J.C.; supervision, K.-H.S. and C.-J.C. All authors have read and agreed to the published version of the manuscript.

Funding: This research was supported by Korea Electric Power Corporation. (Grant number: R20XO02-10), and by Materials/Parts Technology Development Program (20022480) funded By the Ministry of Trade, Industry and Energy (MOTIE, Korea).

Data Availability Statement: No new data were created or analyzed in this study. Data sharing is not applicable to this article.

Conflicts of Interest: The authors declare no conflict of interest. The funding agencies had no role in the decision to publish the results.

References

1. Kushvaha, S.S.; Pal, P.; Shukla, A.K.; Joshi, A.G.; Gupta, G.; Kumar, M.; Singh, S.; Gupta, B.K.; Haranath, D. Effect of growth temperature on defects in epitaxial GaN film grown by plasma assisted molecular beam epitaxy. *AIP Adv.* **2014**, *4*, 027114. [[CrossRef](#)]
2. Qi, M.; Nomoto, K.; Zhu, M.; Hu, Z.; Zhao, Y.; Protasenko, V.; Song, B.; Yan, X.; Li, G.; Verma, J.; et al. High breakdown single-crystal GaN pn diodes by molecular beam epitaxy. *Appl. Phys. Lett.* **2015**, *1072*, 32101. [[CrossRef](#)]
3. Alam, M.D.; Gaevski, M.; Jewel, M.U.; Mollah, S.; Mamun, A.; Hussain, K.; Floyd, R.; Simin, G.; Chandrashekar, M.V.S.; Khan, A. Excimer laser liftoff of AlGaIn/GaN HEMTs on thick AlN heat spreaders. *Appl. Phys. Lett.* **2021**, *119*, 132106. [[CrossRef](#)]
4. Chen, H.; Tang, N.; Zuo, Z. Improvement and Reduction of Self-Heating Effect in AlGaIn/GaN HEMT Devices. *J. Sens.* **2022**, *10*, 1–10. [[CrossRef](#)]
5. Benzarti, Z.; Sekrafi, T.; Bougrioua, Z.; Khalfallah, A.; El Jani, B. Effect of SiN Treatment on Optical Properties of In_xGa_{1-x}N/GaN MQW Blue LEDs. *J. Electron. Mater.* **2017**, *46*, 4312–4320. [[CrossRef](#)]
6. Wośko, M.; Paszkiewicz, B.; Szymański, T.; Paszkiewicz, R. Comparison of electrical, optical and structural properties of epitaxially grown HEMT's type AlGaIn/AlN/GaN heterostructures on Al₂O₃, Si and SiC substrates. *Superlattices Microstruct.* **2016**, *100*, 619–626. [[CrossRef](#)]
7. Pharkphoumy, S.; Janardhanam, V.; Jang, T.H.; Park, J.; Shim, K.H.; Choi, C.J. Optimized Device Geometry of Normally-On Field-Plate AlGaIn/GaN High Electron Mobility Transistors for High Breakdown Performance Using TCAD Simulation. *Electronics* **2021**, *10*, 2642. [[CrossRef](#)]
8. He, X.G.; Zhao, D.G.; Jiang, D.S. Formation of two-dimensional electron gas at AlGaIn/GaN heterostructure and the derivation of its sheet density expression. *Chin. Phys. B* **2015**, *24*, 067301. [[CrossRef](#)]
9. Rathore, S.U.; Dimitrijević, S.; Amini Moghadam, H.; Mohd-Yasin, F. Equations for the electron density of the two-dimensional electron gas in realistic AlGaIn/GaN heterostructures. *Nanomanufacturing* **2021**, *1*, 12. [[CrossRef](#)]
10. Chang, S.J.; Cho, K.J.; Lee, S.Y.; Jeong, H.H.; Lee, J.H.; Jung, H.W.; Bae, S.B.; Choi, I.G.; Kim, H.C.; Ahn, H.K.; et al. Substrate Effects on the Electrical Properties in GaN-Based High Electron Mobility Transistors. *Crystals* **2021**, *11*, 1414. [[CrossRef](#)]
11. Yusuf, Y.; Samsudin, M.E.A.; Taib, M.I.M.; Ahmad, M.A.; Mohamed, M.F.P.; Kawarada, H.; Falina, S.; Zainal, N.; Syamsul, M. Two-Step GaN Layer Growth for High-Voltage Lateral AlGaIn/GaN HEMT. *Crystals* **2023**, *13*, 90. [[CrossRef](#)]
12. Borga, M.; Meneghini, M.; Rossetto, I.; Stoffels, S.; Posthuma, N.; Van Hove, M.; Marcon, D.; Decoutere, S.; Meneghesso, G.; Zanoni, E. Evidence of time-dependent vertical breakdown in GaN-on-Si HEMTs. *IEEE Trans. Electron Devices* **2017**, *64*, 3616–3621. [[CrossRef](#)]
13. Borga, M.; Meneghini, M.; Stoffels, S.; Van Hove, M.; Zhao, M.; Li, X.; Decoutere, S.; Zanoni, E.; Meneghesso, G. Impact of the substrate and buffer design on the performance of GaN on Si power HEMTs. *Microelectron. Reliab.* **2018**, *88–90*, 584–588. [[CrossRef](#)]
14. Weyher, J.L.; Ashraf, H.; Hageman, P.R. Reduction of dislocation density in epitaxial GaN layers by overgrowth of defect-related etch pits. *Appl. Phys. Lett.* **2009**, *95*, 031913. [[CrossRef](#)]
15. Halidou, I.; Benzarti, Z.; Bougrioua, Z.; Boufaden, T.; El Jani, B. Correlation between morphological, electrical and optical properties of GaN at all stages of MOVPE Si/N treatment growth. *Superlattices Microstruct.* **2006**, *40*, 490–495. [[CrossRef](#)]
16. Boughrara, N.; Benzarti, Z.; Khalfallah, A.; Evaristo, M.; Cavaleiro, A. Comparative study on the nanomechanical behavior and physical properties influenced by the epitaxial growth mechanisms of GaN thin films. *Appl. Surf. Sci.* **2022**, *579*, 152188. [[CrossRef](#)]
17. Wang, X.; Huang, S.; Zheng, Y.; Wei, K.; Chen, X.; Zhang, H.; Liu, X. Effect of GaN channel layer thickness on DC and RF performance of GaN HEMTs with composite AlGaIn/GaN buffer. *IEEE Trans. Electron Devices* **2014**, *61*, 1341–1346. [[CrossRef](#)]
18. Guan, H.; Shen, G.; Liu, S.; Jiang, C.; Wu, J. A Simulation Optimization Factor of Si (111)-Based AlGaIn/GaN Epitaxy for High Frequency and Low-Voltage-Control High Electron Mobility Transistor Application. *Micromachines* **2023**, *14*, 168. [[CrossRef](#)]
19. Singhal, J.; Chaudhuri, R.; Hickman, A.; Protasenko, V.; Xing, H.G.; Jena, D. Toward AlGaIn channel HEMTs on AlN: Polarization-induced 2DEGs in AlN/AlGaIn/AlN heterostructures. *APL Mater.* **2022**, *10*, 111120. [[CrossRef](#)]

20. Green, B.M.; Chu, K.K.; Chumbes, E.M.; Smart, J.A.; Shealy, J.R.; Eastman, L.F. The effect of surface passivation on the microwave characteristics of undoped AlGaIn/GaN HEMTs. *IEEE Electron Device Lett.* **2000**, *21*, 268–270. [[CrossRef](#)]
21. Vetry, R.; Zhang, N.Q.; Keller, S.; Mishra, U.K. The impact of surface states on the DC and RF characteristics of AlGaIn/GaN HFETs. *IEEE Trans. Electron Devices* **2001**, *48*, 560–566. [[CrossRef](#)]
22. Adivarahan, V.; Simin, G.; Yang, J.W.; Lunev, A.; Khan, M.A.; Pala, N.; Shur, M.; Gaska, R. SiO₂-passivated lateral-geometry GaN transparent Schottky-barrier detectors. *Appl. Phys. Lett.* **2000**, *77*, 863–865. [[CrossRef](#)]
23. Xing, H.; Dora, Y.; Chini, A.; Heikman, S.; Keller, S.; Mishra, U.K. High breakdown voltage AlGaIn-GaN HEMTs achieved by multiple field plates. *IEEE Electron Device Lett.* **2004**, *25*, 161–163. [[CrossRef](#)]
24. Wang, W.K.; Lin, C.H.; Lin, P.C.; Lin, C.K.; Huang, F.H.; Chan, Y.J.; Chen, G.T.; Chyi, J.I. Low- κ /BCB passivation on AlGaIn-GaN HEMT fabrication. *IEEE Electron Device Lett.* **2004**, *25*, 763–765. [[CrossRef](#)]
25. Kang, M.J.; Kim, H.S.; Cha, H.Y.; Seo, K.S. Development of Catalytic-CVD SiN_x Passivation Process for AlGaIn/GaN-on-Si HEMTs. *Crystals* **2020**, *10*, 842. [[CrossRef](#)]
26. Huang, C.Y.; Mazumder, S.; Lin, P.C.; Lee, K.W.; Wang, Y.H. Improved Electrical Characteristics of AlGaIn/GaN High-Electron-Mobility Transistor with Al₂O₃/ZrO₂ Stacked Gate Dielectrics. *Materials* **2022**, *15*, 6895. [[CrossRef](#)] [[PubMed](#)]
27. Khan, M.A.; Hu, X.; Sumin, G.; Lunev, A.; Yang, J.; Shur, M.S. AlGaIn/GaN metal oxide semiconductor heterostructure field effect transistor. *IEEE Electron Device Lett.* **2000**, *21*, 63–65. [[CrossRef](#)]
28. Ha, M.W.; Lee, S.C.; Park, J.H.; Her, J.C.; Seo, K.S.; Han, M.K. Silicon dioxide passivation of AlGaIn/GaN HEMTs for high breakdown voltage. In Proceedings of the 2006 IEEE International Symposium on Power Semiconductor Devices and IC's, Naples, Italy, 4–8 June 2006; IEEE: Piscataway, NJ, USA, 2006; pp. 1–4. [[CrossRef](#)]
29. Geng, K.; Chen, D.; Zhou, Q.; Wang, H. AlGaIn/GaN MIS-HEMT with PECVD SiN_x, SiON, SiO₂ as gate dielectric and passivation layer. *Electronics* **2018**, *7*, 416. [[CrossRef](#)]
30. Arulkumar, S.; Egawa, T.; Ishikawa, H.; Jimbo, T.; Sano, Y. Surface passivation effects on AlGaIn/GaN high-electron-mobility transistors with SiO₂, Si₃N₄, and silicon oxynitride. *Appl. Phys. Lett.* **2004**, *84*, 613–615. [[CrossRef](#)]
31. Boughrara, N.; Benzarti, Z.; Khalfallah, A.; Oliveira, J.C.; Evaristo, M.; Cavaleiro, A. Thickness-dependent physical and nanomechanical properties of Al_xGa_{1-x}N thin films. *Mater. Sci. Semicond. Process.* **2022**, *151*, 107023. [[CrossRef](#)]
32. Gupta, A.; Chatterjee, N.; Kumar, P.; Pandey, S. Effect of surface passivation on the electrical characteristics of nanoscale AlGaIn/GaN HEMT. *IOP Conf. Ser. Mater. Sci. Eng.* **2017**, *225*, 012095. [[CrossRef](#)]
33. Mukhopadhyay, P.; Bag, A.; Gomes, U.; Banerjee, U.; Ghosh, S.; Kabi, S.; Chang, E.Y.; Dabiran, A.; Chow, P.; Biswas, D. Comparative DC characteristic analysis of AlGaIn/GaN HEMTs grown on Si (111) and sapphire substrates by MBE. *J. Electron. Mater.* **2014**, *43*, 1263–1270. [[CrossRef](#)]
34. Ji, H.; Das, J.; Germain, M.; Kuball, M. Laser lift-off transfer of AlGaIn/GaN HEMTs from sapphire onto Si: A thermal perspective. *Solid-State Electron.* **2009**, *53*, 526–529. [[CrossRef](#)]
35. Nigam, A.; Bhat, T.N.; Rajamani, S.; Dolmanan, S.B.; Tripathy, S.; Kumar, M. Effect of self-heating on electrical characteristics of AlGaIn/GaN HEMT on Si (111) substrate. *AIP Adv.* **2017**, *7*, 085015. [[CrossRef](#)]
36. Asubar, J.T.; Yatabe, Z.; Hashizume, T. Reduced thermal resistance in AlGaIn/GaN multi-mesa-channel high electron mobility transistors. *Appl. Phys. Lett.* **2014**, *105*, 053510. [[CrossRef](#)]
37. Song, L.; Fu, K.; Zhang, Z.; Sun, S.; Li, W.; Yu, G.; Hao, R.; Fan, Y.; Shi, W.; Cai, Y.; et al. Interface Si donor control to improve dynamic performance of AlGaIn/GaN MIS-HEMTs. *AIP Adv.* **2017**, *7*, 125023. [[CrossRef](#)]
38. Ha, M.W.; Choi, Y.H.; Park, J.H.; Seo, K.S.; Han, M.K. Hot Carrier Stress Effects of SiO₂ Passivated AlGaIn/GaN High Electron Mobility Transistors. *ECS Trans.* **2006**, *3*, 213–220. [[CrossRef](#)]
39. Wu, Q.; Xu, Y.; Zhou, J.; Kong, Y.; Chen, T.; Wang, Y.; Lin, F.; Fu, Y.; Jia, Y.; Zhao, X.; et al. Performance comparison of GaN HEMTs on diamond and SiC substrates based on surface potential model. *ECS J. Solid State Sci. Technol.* **2017**, *6*, Q171–Q178. [[CrossRef](#)]
40. Jin, D.; del Alamo, J.A. Mechanisms responsible for dynamic ON-resistance in GaN high-voltage HEMTs. In Proceedings of the 2012 24th International Symposium on Power Semiconductor Devices and ICs, Bruges, Belgium, 3–7 June 2012; pp. 333–336. [[CrossRef](#)]
41. Ng, T.K.; Holguin-Lerma, J.A.; Kang, C.H.; Ashry, I.; Zhang, H.; Bucci, G.; Ooi, B.S. Group-III-nitride and halide-perovskite semiconductor gain media for amplified spontaneous emission and lasing applications. *J. Phys. D Appl. Phys.* **2021**, *54*, 143001. [[CrossRef](#)]
42. Guillén-Cervantes, A.; Rivera-Álvarez, Z.; López-López, M.; Ponce-Pedraza, A.; Guarneros, C.; Sánchez-Reséndiz, V.M. Structural and optical properties of GaN thin films grown on Al₂O₃ substrates by MOCVD at different reactor pressures. *Appl. Surf. Sci.* **2011**, *258*, 1267–1271. [[CrossRef](#)]
43. Liu, A.C.; Tu, P.T.; Langpoklakpam, C.; Huang, Y.W.; Chang, Y.T.; Tzou, A.J.; Hsu, L.H.; Lin, C.H.; Kuo, H.C.; Chang, E.Y. The evolution of manufacturing technology for GaN electronic devices. *Micromachines* **2021**, *12*, 737. [[CrossRef](#)] [[PubMed](#)]

Disclaimer/Publisher's Note: The statements, opinions and data contained in all publications are solely those of the individual author(s) and contributor(s) and not of MDPI and/or the editor(s). MDPI and/or the editor(s) disclaim responsibility for any injury to people or property resulting from any ideas, methods, instructions or products referred to in the content.